Environmental Toxicology and Chemistry—Volume 41, Number 6—pp. 1439–1450, 2022
Received: 5 October 2021 | Revised: 17 December 2021 | Accepted: 24 February 2022

Environmental Toxicology

Development of a Quasi–Quantitative Structure–Activity Relationship Model for Prediction of the Immobilization Response of *Daphnia magna* Exposed to Metal-Based Nanomaterials

Warisa Bunmahotama,[a] Martina G. Vijver,[a] and Willie Peijnenburg[a,b,*]

[a]Institute of Environmental Sciences, Leiden University, Leiden, The Netherlands
[b]Center for Safety of Substances and Products, National Institute of Public Health and the Environment, Bilthoven, The Netherlands

Abstract: The conventional Hill equation model is suitable to fit dose–response data obtained from performing (eco)toxicity assays. Models based on quasi–quantitative structure–activity relationships (QSARs) to estimate the Hill coefficient (n_H) were developed with the aim of predicting the response of the invertebrate species *Daphnia magna* to exposure to metal-based nanomaterials. Descriptors representing the pristine properties of nanoparticles and media conditions were coded to a quasi–simplified molecular input line entry system and correlated to experimentally derived values of n_H. Monte Carlo optimization was used to model the set of n_H values, and the model was trained on the basis of reported dose–response relationships of 60 data sets ($n = 367$ individual response observations) of 11 metal-based nanomaterials as obtained from 20 literature reports. The model simulates the training data well, with only 2.3% deviation between experimental and modeled response data. The technique was employed to predict the dose–response relationships of 15 additional data sets ($n = 72$ individual observations) not included in model development of seven metal-based nanomaterials from 10 literature reports, with an average error of 3.5%. Combining the model output with either the median effective concentration value or any other known effect level as obtained from experimental data allows the prediction of full dose–response curves of *D. magna* immobilization. This model is an accurate screening tool that allows the determination of the shape and slope of dose–response curves, thereby greatly reducing experimental effort in case of novel advanced metal-based nanomaterials or the prediction of responses in altered exposure media. This screening model is compliant with the 3Rs (replacement, reduction, and refinement) principle, which is embraced by the scientific and regulatory communities dealing with nano-safety. *Environ Toxicol Chem* 2022;41:1439–1450. © 2022 The Authors. *Environmental Toxicology and Chemistry* published by Wiley Periodicals LLC on behalf of SETAC.

Keywords: Toxicity; Hill equation; Nanoparticles; Invertebrates; Modeling

INTRODUCTION

Engineered nanomaterials (ENMs) are widely applied, in areas varying from healthcare, agriculture, transport, and energy to advanced materials. The worldwide production capacity of ENMs was estimated to be 50,000 tons per year in 2020 (Heggelund et al., 2014). It is reasonable to expect that many of these ENMs end up in natural water systems, and hazard and risk assessment frameworks are to be put into place to estimate potential risks. The notion that nanomaterials' distinct features compared to larger counterparts should be considered in safety assessment has led to the development of risk-assessment frameworks that are specific to nanomaterials as well as to testing protocols that account for nano-specific features (Oomen et al., 2018). One of the representative invertebrate species in this respect is the crustacean species *Daphnia magna*. Tests with *D. magna* are fully standardized within the Organisation for Economic Co-operation and Development (OECD) guidance documents (OECD, 2004) and modified for nanomaterials (the so-called NanoReg protocols

This article contains online-only Supporting Information.

* Address correspondence to willie.peijnenburg@rivm.nl
Published online 2 March 2022 in Wiley Online Library (wileyonlinelibrary.com).
DOI: 10.1002/etc.5322

[Jantunen et al., 2018]). The typical test outcome is the full dose–response relationship, describing the magnitude of the response as a function of exposure concentration. In the case of daphnids, immobilization is commonly used as the endpoint.

At least 200 studies have been published in recent years on daphnids exposed to a variety of (single) metal-based nanomaterials (Chen et al., 2015). Although many data points are available, no systematic model has been developed so far based on the available set of data and with the specific aim of predicting the full dose–response curves of metal-based ENMs. Because various metal-based ENMs are of major environmental concern, a predictive model intended for approximating the dose–response relationship of these ENMs against *D. magna* immobilization would be exceptionally valuable. In addition, this model would allow for screening untested or randomly tested metal-based nanomaterials, whereas the model would also allow the prioritization of nanomaterials for which experimental data should be collected more systematically. Thereupon, the model would be instrumental to environmental effect assessment and would comply with the 3Rs (replacement, reduction, and refinement) principle developed over 50 years ago, providing a framework for performing more humane animal testing.

The aim of the present study was to develop a model to allow prediction of the dose–response relationship of a variety of metal-based nanomaterials. The focus is on the shape of the dose–response curve for the commonly used laboratory test organism *D. magna*, using immobilization as the endpoint. To address this aim, (1) experimental data were collected on the acute toxicity of daphnids to various metal-based nanomaterials tested under different conditions; (2) based on the Hill equation (Hill, 1910), the relationship between the dose of the nanosuspension and the immobilization response data was calculated; and (3) a quasi–quantitative structure–activity relationship (QSAR) model was developed to estimate the calculated relationships based on specific nanomaterial properties. Ultimately, this mathematical estimation has the prospect of leading to a user-friendly model allowing calculation of the full dose–response curve when only one effective concentration (EC) value is reported. This way, the model assists in nanosafety assessment and is instrumental to efficiently prioritize, rank, and group nanomaterials.

METHODS

Data selection and collection

Data were collected making use of different databases, including the data entries from the Web of Science Core Collection with bibliometric data search as described in Chen et al. (2015). The Boolean operators were (TS = ["*toxicity" AND "effect*"] AND TI = ["nano"] AND KP = [nano* AND metal* OR "nano* AND metal oxide*"] AND KP = [crustacea* OR daphni*]) AND LANGUAGE: (English) AND DOCUMENT TYPES: (Article), with a time span of 2005–2020. In addition, a literature search was done in Google Scholar (2005–2020) using the following keywords: "toxicity," "effect," "nano," "metal," "metal oxide," "crustacea," and "daphni." This search yielded 1001 records overall. Of these records, for 20 reports corresponding with 75 records, the full dose–response curve was published (the criterion used to define a full dose–response curve was that four or more data points were experimentally quantified), and these data were selected as the basis of the databases. Model validation was performed using a subset of 10 reports.

The database consisted of data with 11 different metal-based nanomaterials and included all pristine nano-properties and exposure conditions. A detailed overview is given in Supporting Information, Tables S1 and S2. In brief, dose–response relationship data on *D. magna* immobilization were retrieved from 20 reports: Briffa et al. (2018), Cui et al. (2017), Cupi et al. (2016), Dabrunz et al. (2011), Heinlaan et al. (2008), Kim et al. (2017), Lee et al. (2012), Ma et al. (2012), Newton et al. (2013), Oleszczuk et al. (2015), Santos-Rasera et al. (2019), Schiwy et al. (2016), Seo et al. (2014), Song et al. (2015), Sovová et al. (2009), Strigul et al. (2009), Wyrwoll et al. (2016), Xiao et al. (2015, 2016), and Yang et al. (2014). The detailed information of each record of ENM, like size and coating, test duration, illumination, and media composition is listed in Supporting Information, Tables S1 and S2. The pristine characteristics of the ENMs (i.e., shape, impurity, surface area, and crystallinity), the characteristics of the ENMs in the test environment (i.e., hydrodynamic size, dissolution, and zeta potential) and acute toxicity values (i.e., whole data set of dose–response relationships including median EC [EC50]) are provided in the Supporting Information.

Hill equation

The Hill coefficient, n_H, that is, the steepness and shape of the response curve which was introduced as an empirical description by Hill (1910), is typically used to quantify the response of a receptor to a stressor (Goldbeter & Dupont, 1990). It is a sigmoidal function commonly prescribed in the OECD guidance document on testing chemicals and nanomaterials (OECD, 2020). The Hill equation is quite often utilized to predict the dose–response relationship of ENMs to a variety of different organisms and different metal-based ENMs, for example, among anatase and rutile $nTiO_2$ to algae (Gao et al., 2020; Li et al., 2015), nCu to bacteria (Chatterjee et al., 2014), and $nTiO_2$ to crustaceans (Farner et al., 2019). The Hill equation (Hill, 1910) was used in the present study:

$$E = \frac{100}{1 + \left(\frac{\mathrm{EC50}}{[\mathrm{A}]}\right)^{n_H}} \quad (1)$$

The Hill equation requires only three parameters to determine the dose–response relationship. In the equation, n_H may be considered as the parameter that is dependent on the characteristics of the ENMs to which the biota are exposed, E is the magnitude of the response, [A] is the number concentration of ENM particles (per liter), and EC50 is the number of ENM particle (per liter) that produces a 50% response. The values of n_H used in the Monte Carlo optimization were obtained

from fitting dose–response relationships for 11 metal-based nanomaterials (60 data sets, $n = 367$ individual observations) from 20 reports listed in Supporting Information, Table S1, using the Hill equation (Equation 1), and the EC50 values that were given in the reports.

The assumptions underlying the Hill equation model are (1) that there is a dose–response relationship and that the shape of this relationship is dependent on the intrinsic characteristics of the ENMs tested, and (2) that the shape of the dose–response curve is independent of the water chemistry conditions tested. Please note that the latter assumption implies that the impact of varying water chemistry is assumed to be reflected in a shift of the dose–response curves, whereas the shape of the curve is assumed to stay unchanged.

Quasi-QSAR model

The quasi-QSAR model was developed with the so-called quasi–simplified molecular input line entry system (SMILES) approach (Toropova et al., 2011). Quasi-SMILES is a string using physicochemical features and/or biochemical conditions as a replacement for conventional SMILES (Choi et al., 2019). The quasi-SMILES-based QSAR model can be demonstrated by the following equation:

$$n_H = C0 + C1 \times DCW(T, N_{Epoch}) \quad (2)$$

In Equation 2, C0 and C1 are the intercept and the slope. The correlation weight of the descriptor (DCW) is computed using the following equation:

$$DCW(T, N_{Epoch}) = \alpha\sum CW(S_k) + \beta\sum CW(SS_k) + \gamma \times CW(NOSP) \quad (3)$$

In Equation 3, S_k and SS_k are SMILES attributes which contain one and two SMILES elements, respectively; $CW(S_k)$ and $CW(SS_k)$ are the correlation weights of the SMILES attributes; NOSP is an index which represents the presence or absence of chemical elements, that is, nitrogen, oxygen, sulfur, and phosphorus; α, β, and γ are coefficients that can be either 1 or 0, with 1 indicating that the SMILES attribute is involved in the calculation of the $DCW(T, N_{Epoch})$ and 0 indicating that the SMILES attribute is not involved; and $DCW(T, N_{Epoch})$, that is, combinations of these values, represents the probability of defining diverse versions of the SMILES-based optimal descriptor (for more detailed information, see, e.g., Carnesecchi et al., 2020; Toropov et al., 2011, 2012; Toropova et al., 2011, 2012). Note that the threshold (T) and the number of epochs (N_{Epoch}) are parameters of the optimization that determine the preferred statistical quality of the training set. To develop the quasi-QSAR models, CORAL software (http://www.insilico.eu/coral) was employed.

The quasi-SMILES employed in the present study was composed of three components:

1. One code to represent the size of the ENMs. The code for ENM size was assigned as a rounded number of nanoparticle diameter (nanometers) to an integer.
2. One code to represent the test conditions, the exposure duration, and/or the presence of a coating on the ENM. The code for representing a toxicity assay and/or ENM coating was a combination of number and plus signs (i.e., 1+, 1++, 1+++), a numeral notation ranging from 1 to 20 was used to represent the 20 reports listed in Supporting Information, Tables S1 and S2, and the number of plus signs represents the number of variations of the toxicity assay/ENM coatings in the report.
3. One code for the ENM type.

A combination of number, symbol, and SMILES was used to build up the quasi-QSAR string. The code for indicating the type of ENMs employed the SMILES line notation that was obtained from the PubChem online database (PubChem, 2021). To compose the quasi-QSAR string, dots "." and parentheses "()" were used as a conjunction between the three components. The quasi-SMILES strings belonging to the *D. magna* immobilization data after exposure to metal-based nanomaterials are listed in Table 1.

Monte Carlo optimization based on repeated random sampling in the CORAL package was employed to optimize the parameters that were descriptive in the quasi-QSAR model and to make numerical estimations of unknown parameters (Metropolis & Ulam, 1949; Rubinstein & Kroese, 2016). The number of random samplings within the Monte Carlo algorithm was set on a maximum of 60 data sets, and the optimization of the quasi-QSAR string was reached to provide a value of R^2 of 0.82. In the present study, the optimization represented correlations between the fitted n_H and the quasi-QSAR string, the correlation weights of which are estimated as $DCW(T, N_{Epoch})$ in Equation 2. In addition, the intercept (C0) and slope (C1) of the quasi-QSAR model in Equation 2 are approximated by the CORAL software.

Verification of the quasi-QSAR

To relate the fitted Hill equation to measured dose–response curves, the percentage of sample deviation (SDEV), as suggested in Crittenden et al. (1999), was adopted. The relative error between experimental data and the model simulation/prediction was employed to illustrate the fit between the model and the experimental data, which is stated as

$$\%\ SDEV = \sqrt{\left[\frac{\sum\left(\frac{P_{model\ calculation} - P_{experimental\ data}}{P_{experimental\ data}}\right)^2}{N_{data} - 1}\right]} \times 100 \quad (4)$$

where $P_{model\ calculation}$ and $P_{experimental\ data}$ are the log of the toxicity value (particles per liter) determined from the simulation/prediction and the individual experimental response

TABLE 1: Fitted and calculated values of n_H for all 75 dose–response relationships studied

Identifier	Quasi-SMILES string	Fitted n_H	Calculated n_H	Error (%)
Simulation set				
+1	(6.1+)O=[Ce]=O	6.2	5.3	17.5
+2	(5.1+)O=[Zn]	2.6	2.4	7.5
+3	(57.2+)[Ag]	7.4	7.8	5.2
+4	(57.2++)[Ag]	6.4	7.9	18.2
+5	(18.3+)[Ag]	4.9	5.2	5.0
+6	(18.3++)[Ag]	4.3	5.2	17.2
+7	(151.3+)O=[Zn]	4.0	1.8	124.0
+8	(151.3++)O=[Zn]	0.9	1.8	49.7
+10	(6.4+)O=[Ti]=O	0.8	1.6	51.2
+11	(6.4++)O=[Ti]=O	2.9	1.6	76.4
+12	(60.5+)O=[Zn]	0.8	1.9	55.9
+13	(30.5+)O=[Cu]	1.4	−0.3	560.5
+14	(40.6++)O=[Cu]	1.5	2.5	39.4
+15	(40.6+++)O=[Cu]	2.5	2.5	0.6
+16	(25.6+)O=[Zn]	2.2	2.8	20.7
+18	(25.6+++)O=[Zn]	2.2	2.9	24.4
+19	(80.7+)[Ag]	22.5	21.0	7.4
+20	(13.7+)[Ag]	25.1	23.6	6.2
+21	(21.8+)O=[Ti]=O	2.1	0.7	197.4
+22	(21.8++)O=[Ti]=O	0.8	0.7	9.3
+23	(6.9+)[Ag]	10.8	9.3	15.8
+24	(5.9++)[Ag]	16.7	9.6	73.5
+25	(25.9+++)[Ag]	2.3	8.3	72.3
+26	(6.9++++)[Ag]	5.8	9.4	38.7
+28	(25.9++++++)[Ag]	6.0	8.4	29.2
+29	(6.9+++++++)[Ag]	11.7	9.5	22.7
+30	(5.9+++++++++)[Ag]	5.9	9.8	40.1
+31	(25.9++++++++++)[Ag]	15.2	8.5	77.6
+32	(100.10+)O=[Zn]	0.9	0.8	25.9
+34	(100.10+++)O=[Zn]	0.5	0.8	41.1
+35	(100.10++++)O=[Zn]	0.5	0.9	36.6
+36	(21.10+)O=[Ti]=O	0.2	−0.2	244.8
+37	(100.10+)[Ni]	0.3	−1.0	134.7
+38	(80.11+)O=[Cu]	4.0	7.3	45.1
+39	(40.11+)O=[Cu]	4.1	2.2	88.4
+40	(25.11+)O=[Cu]	3.0	2.1	41.2
+41	(62.12+)O=[Fe]O[Fe]=O	1.0	1.0	0.2
+42	(15.13+)[Ag]	3.9	5.9	33.2
+43	(15.13++)[Ag]	3.5	5.9	41.1
+45	(40.13+)O=[Cu]	1.4	1.1	34.0
+47	(40.13+++)O=[Cu]	1.2	1.1	6.8
+48	(25.13+)O=[Zn]	1.9	1.5	28.0
+49	(25.13++)O=[Zn]	2.7	1.5	77.4
+50	(25.13+++)O=[Zn]	2.0	1.5	28.9
+51	(25.14+)[Cu]	3.9	4.3	8.4
+52	(50.14+)[Cu]	5.6	5.5	2.2
+54	(50.15+)O=[Cu]	1.4	1.8	22.7
+56	(15.16++)[B]	2.8	0.9	207.0
+57	(100.16+++)[Al]	0.9	0.5	77.7
+59	(100.16+++++)[Al]	0.3	0.6	50.7
+62	(210.17+)O=[Ti]=O	3.6	4.8	24.8
+64	(9.17+++)O=[Ti]=O	1.8	3.3	46.2
+65	(20.17+++)O=[Ti]=O	1.0	0.5	113.1
+67	(43.18+)O=[Zn]	3.5	5.3	33.8
+69	(50.19++)[Cu]	4.3	3.7	18.2
+70	(50.19+++)[Cu]	1.6	3.7	56.4
+71	(50.19++++)[Cu]	7.1	3.7	90.5
+72	(50.19+++++)[Cu]	3.2	3.8	16.0
+73	(50.19++++++)[Cu]	2.3	3.8	38.8
+75	(15.20+)O=[Si]=O	0.7	0.7	6.5
Prediction set				
#9	(25.3+)O=[Ti]=O	–	3.1	–
#17	(25.6++)O=[Zn]	–	2.9	–
#27	(5.9+++++)[Ag]	–	9.7	–
#33	(100.10++)O=[Zn]	–	0.8	–
#44	(15.13+++)[Ag]	–	6.0	–
#46	(40.13++)O=[Cu]	–	1.1	–
#53	(100.14+)[Cu]	–	4.2	–
#55	(15.16+)[B]	–	0.9	–
#58	(100.16++++)[Al]	–	0.6	–
#60	(9.17+)O=[Ti]=O	–	3.2	–
#61	(20.17+)O=[Ti]=O	–	0.4	–
#63	(9.17++)O=[Ti]=O	–	3.3	–
#66	(50.18+)[Cu]	–	2.1	–
#68	(50.19+)[Cu]	–	3.6	–
#74	(50.19+++++++)[Cu]	–	3.8	–

n_H = Hill coefficient; SMILES = simplified molecular input line entry system.

data for various magnitudes of the response, respectively, and N_{data} is the number of data. Model simulation/predictions include data restricted to the EC5–EC95 range because outside this range the experimental noise is relatively large (Chevalier, 2014), making the experimental data less robust for model-building.

RESULTS AND DISCUSSION

Descriptive analysis of data

Experimental data on the acute toxicity of daphnids to various metal-based nanomaterials tested ranged between 7.74×10^5 and 8.54×10^{16} particles/L, hence an immense difference of 11 orders of magnitude. All retrieved acute toxicity data on the endpoint immobilization of daphnids within a 24–96-h exposure duration were used. Metal-based nanomaterials were predominantly tested as bare particles (59 cases). A coating on the particles was applied in 16 cases, the coating being a mixture of polyvinylpyrrolidone coatings, gum arabic coatings, polyethylene glycol coatings, aluminum oxide coatings, and carboxylate ligand coating. The size of the nanomaterials and their agglomerates ranged from 4.7 to 210 nm and from 20.6 nm to 500 μm, respectively. The zeta potential, indicative of the stability of the particles in suspension, was measured within the majority of studies (80%) and ranged between 60 and −45.2 mV. Hence, stable and non-stable particles were present in the suspensions in which the daphnids were exposed. All data and details are openly accessible via the Supporting Information.

Dose–response modeling

Typical dose–response curves for different metals are provided in Figure 1A,B. The dose is expressed in the figure in units of the log-transformed number of particles per liter on the *x*-axis and the immobilization response (percentage) on the *y*-axis. The slope of the dose–response curves is dependent of the type of nanoparticulate metals in the suspension, as can be seen from comparing the dose–response curves for nAg,

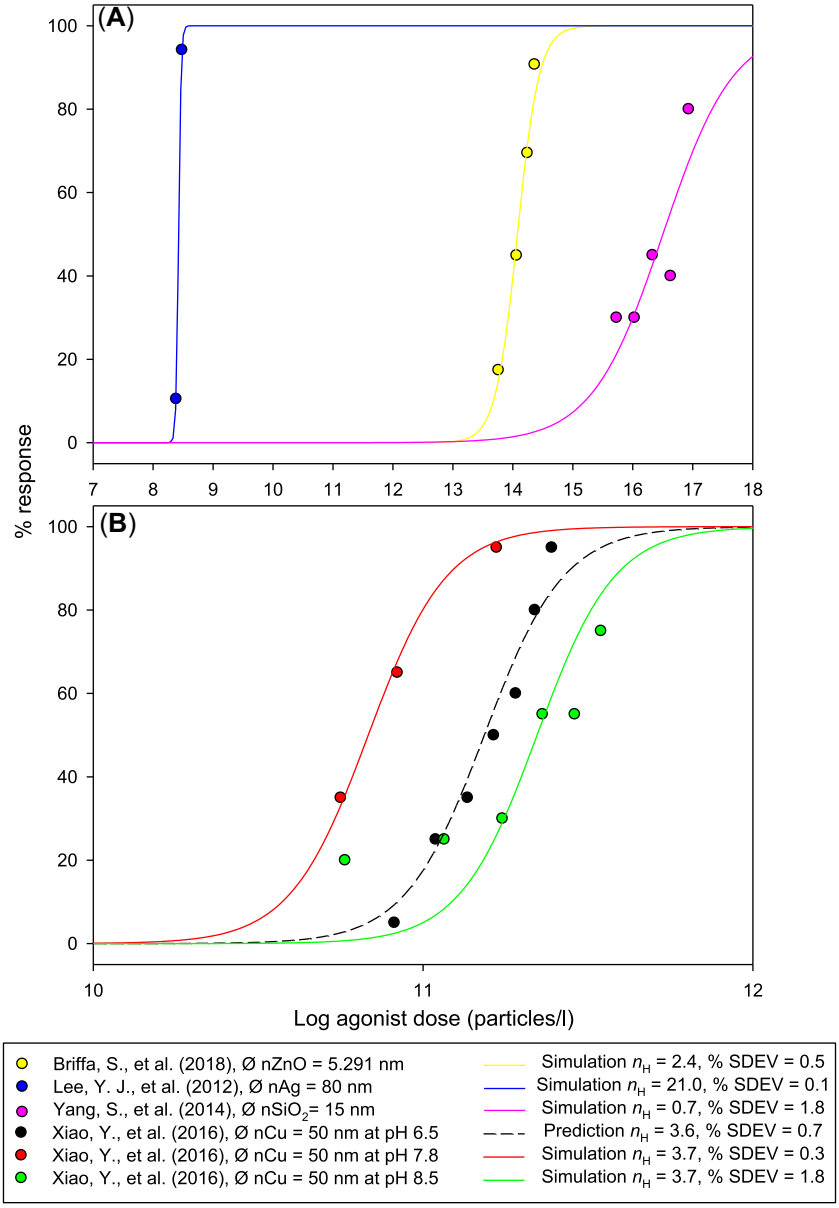

FIGURE 1: Modeled dose–response curves for *Daphnia magna* immobilization, where (**A**) shows the model simulations for three metal-based nanomaterials, that is, nZnO, nAg, and $nSiO_2$. The experimental data were retrieved from Briffa et al. (2018), Lee et al. (2012), and Yang et al. (2014). (**B**) Model simulations and predictions for nCu at three pH values, that is, 6.5, 7.8, and 8.5, for which the data were reported by Xiao et al. (2016).

$nSiO_2$, and nZnO in Figure 1A. The fitted n_H values for nZnO, nAg, and $nSiO_2$ are 2.6, 22.5, and 0.7, respectively. Details on the fitted dose–response curves, with an average R^2 of 0.95, are provided in the Supporting Information. As shown in Figure 1A and as can be deduced from the percentage of SDEV, the models fitted the data well with an average SDEV of 0.8%. The simulated n_H values by the quasi-QSAR model for these three metal-based ENMs were significantly different, that is, 2.4, 21.0, and 0.7 for nZnO, nAg, and $nSiO_2$, respectively.

The Hill coefficient is the parameter that is dependent primarily on the characteristics of the ENM to which the biota are exposed. We therefore assumed that for different chemistry conditions the Hill coefficient remains the same. This assumption is confirmed by the dose–response curves obtained for nCu exposure at different pH values. As shown in Figure 1B, it can first of all be concluded that the quasi-QSAR model fitted the data well with an average SDEV of 0.9%. The simulated (indicating that the experiment at pH 6.5 was randomly included in the data set used for model development) and predicted (indicating that the experiments at pH 7.8 and 8.5 were included in the data set used for model validation) n_H values for the three pH values were very close, that is, 3.6, 3.7, and 3.7 for pH 6.5, 7.8, and 8.5, respectively. The quasi-QSAR descriptors gave a good fit of the overall set of dose–response data with an average R^2 of 0.93.

Another example of showcasing the typical accuracy of the fitted n_H values concerns the case of nZnO. Dose–response data for nZnO of different sizes and coatings were obtained from seven literature sources: Briffa et al. (2018), Cupi et al. (2016), Heinlaan et al. (2008), Kim et al. (2017), Oleszczuk et al.

(2015), Seo et al. (2014), and Xiao et al. (2015). The fitted values of the experimental dose–response data yielded values of n_H which ranged from 0.5 to 4.0 with an average R^2 of 0.91. The quasi-QSAR model calculated a value of n_H of 2.4, which is well within the range of experimental values. Another example relates to the fitted values of n_H for nAg. The underlying data were retrieved from five literature sources (Cui et al., 2017; Cupi et al., 2016; Lee et al., 2012; Newton et al., 2013; Seo et al., 2014), and the values of n_H ranged from 2.3 to 25.1 with an average R^2 of the fit of the dose–response data of 0.97. Our quasi-QSAR model calculated an n_H value for nAg of 21.0. The finding that the modeled n_H values for nCu, nZnO, and nAg are very similar to the values fitted from dose–response data suggests that the present approach provides a proper computational means to calculate n_H for metal-based ENMs under different conditions. It is to be noted that the large variation of the fitted n_H values of nAg might be related to differences in the stability of the nanosuspensions, as can be deduced from the values of the zeta potential. In a high-hardness exposure media, the nAg particles (this specific data set is included in the data set given in Supporting Information, Table S1, as experiment "+20 of nAg Ø 13.3 nm") had a zeta potential of −45.2 mV, and the fitted n_H value was equal to 25.1 ($R^2 = 0.99$). The nAg in a moderate-hardness exposure media (experiment "+42 of nAg Ø 15 nm" in the Supporting Information) was reported to have a zeta potential of -22.5 ± 1.2 mV, and the fitted n_H value was equal to 3.9 ($R^2 = 0.99$). Values of the zeta potential of more than +30 mV or less than −30 mV are commonly considered as being indicative of electrostatic stabilization of nanoparticle suspensions (Honary & Zahir, 2013a, 2013b), which in turn warrants lack of particle aggregation. Lack of aggregation maximizes the potential for uptake of the stabilized particles and the likelihood of adverse effects on *D. magna* (Panzarini et al., 2018), hence yielding a steeper dose–response curve in the case of stabilized nanoparticles at the same exposure doses.

Predictions and simulations of the dose–response relationships

Figures 2 and 3 show examples of the model simulations and predictions of the dose–response curves for different metal-based nanomaterials and environmental conditions against *D. magna* immobilization. The term *model simulations* refers to data used for model development, and the term *predictions* refers to the model application for a data set not included in model development. Modeled dose–response curves are shown in Figure 2 for three metal-based nanomaterials: nAg, nCuO, and nZnO. The data were obtained using the same experimental conditions (OECD test guideline no. 202 [OECD, 2004], 20 ± 2 °C and 16:8-h light: dark cycle) with three different media (moderately hard water [International Organization for Standardization, 2012] and hard water), as reported by Seo et al. (2014). Modeled dose–response curves are shown in Figure 3 for the same spherical nCu particle as obtained using the same experimental conditions in seven different exposure media (pH 6.5–8.5 and dissolved organic

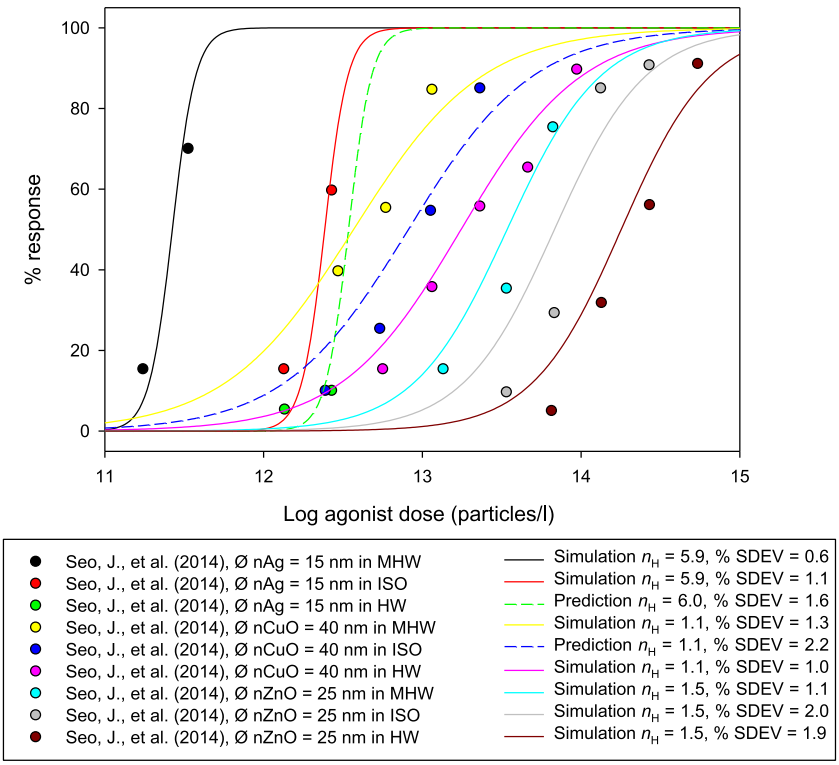

FIGURE 2: Model simulation and prediction of dose–response curves for impacts of three metal-based nanomaterials, that is, nAg, nCuO, and nZnO, on *Daphnia magna* immobilization. Data were obtained from Seo et al. (2014).

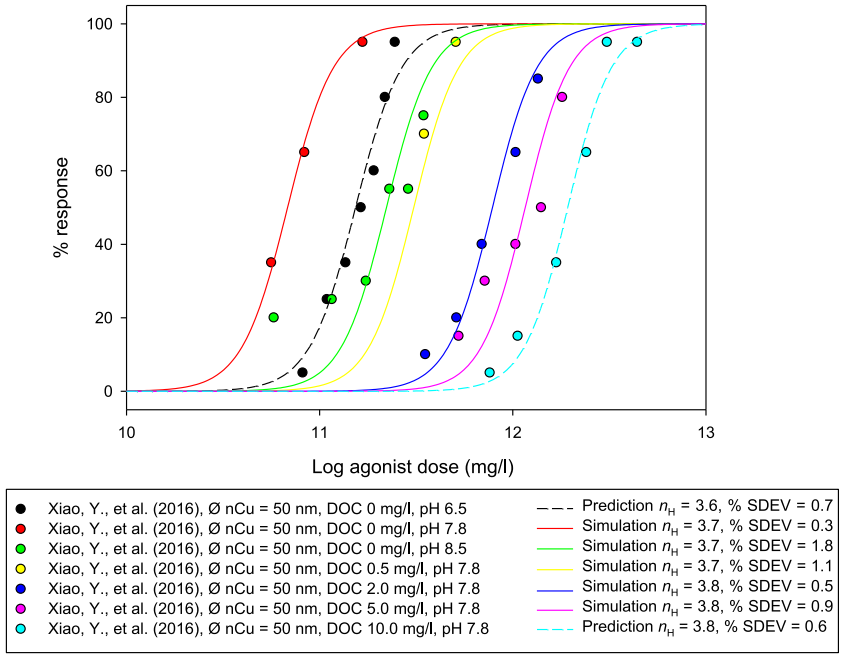

FIGURE 3: Model simulation and prediction of dose–response relationships for impacts of nCu on *Daphnia magna* immobilization. Data were obtained from Xiao et al. (2016).

carbon [DOC] 0–10 mg/L) as reported by Xiao et al. (2016). Figures 2 and 3 demonstrate that the models account for the experimental data reasonably well, with on average 1.2% SDEV. The quasi-QSAR model was further applied to simulate and predict the dose response of the remaining 18 reports, as shown in Supporting Information, Figures S3–S20. The percentage SDEV for the overall array of 75 data sets (60 simulation sets, 15 prediction sets) is listed in Table 2. Note that the average SDEV of all studied data sets is 2.1%, and 95% of the data sets were successfully modeled with SDEV < 6.0%. It is also to be noted that "N/A" in Table 2 indicates that calculated n_H values were negative. This is either an error of the quasi-QSAR model calculation or an indication of a case where the number of data points was <2 because in the latter case the SDEV cannot be calculated.

Figure 4A,B shows the model simulation and prediction of all individual experimental response data in the data sets presented in Supporting Information, Tables S1 and S2, respectively. The number of data points and the magnitude of the responses are listed in Supporting Information, Table S3. The calculated n_H values of these 75 data sets are listed in Table 1. It is noted that among the 60 data sets (including 11 metal-based nanomaterials: nAg, nAl, nB, $nCeO_2$, nCu, nCuO, nFe, nNi, $nSiO_2$, $nTiO_2$, and nZnO) used in Monte Carlo optimization, three data sets have calculated n_H values that were negative, that is, data sets +13, +36, and +37, which is an error of the quasi-QSAR model calculation. The negative n_H value has no meaning in quantifying the response of a receptor to a stressor because it implies lower responses on increasing external particle concentrations. These data sets were therefore not included in the data set used for evaluating the model simulations. Figure 4A shows a typical model simulation of the dose–response data representing the impacts of 10 metal-based nanomaterials (nAg, nAl, nB, $nCeO_2$, nCu, nCuO, nFe, $nSiO_2$, $nTiO_2$, and nZnO) on *D. magna* immobilization. On the *x*-axes, the dose is expressed as the log-transformed measured dose with units of number of particles per liter. On the *y*-axes, the dose is expressed as the log-transformed simulated or predicted dose in the same units of number of particles per liter. The model was also employed for the prediction of the dose–response curves of a series of new data sets of seven metal-based nanomaterials (nAg, nAl, nB, nCu, nCuO, $nTiO_2$, and nZnO), as shown in Figure 4B. The experimental data were extracted from a subset of 10 reports as listed in Supporting Information, Table S2. In these data sets the relevant exposure dose that covers the 5%–95% response levels of the daphnids ranges from 2.43×10^8 to 8.54×10^{16} particles/L, as listed in the Supporting Information.

The results in Figure 4A,B demonstrate that the model is able to simulate and predict the experimental data well, with an overall 2.7% SDEV ($R^2 = 0.96$). The model performance is as good as the model fitting in the sense that the overall SDEV is equal to 5.7% ($R^2 = 0.94$, $n = 390$), as shown in Supporting Information, Figure S1. The 95% confidence and prediction intervals are shown in Supporting Information, Figure S2.

Applicability and limitations of the model

The quasi-QSAR model developed in the present study has been successfully tested in simulations and predictions of the dose–response relationships of metal-based ENMs against *D. magna* immobilization in various test media. The model

TABLE 2: Summary of the parameters used in the quasi-quantitative structure–activity relationship-Hill model

Identifier	EC50 (particles/L)	Fitted n_H	Number of data points	% SDEV
Simulation set				
+1	14.3	5.3	2	0.2
+2	14.1	2.4	4	0.5
+3	10.7	7.8	4	0.3
+4	10.7	7.9	4	0.4
+5	12.2	5.2	4	0.5
+6	12.4	5.2	4	0.4
+7	9.7	1.8	1	–
+8	11.7	1.8	5	2.6
+10	15.9	1.6	5	2.0
+11	15.2	1.6	2	0.9
+12	12.5	1.9	5	2.0
+13	13.5	–0.3	N/A	N/A
+14	12.7	2.5	5	1.6
+15	12.3	2.5	2	0.5
+16	13.6	2.8	2	2.2
+18	13.4	2.9	2	2.4
+19	8.4	21.0	2	0.1
+20	11.8	23.6	0	–
+21	12.2	0.7	7	4.8
+22	17.0	0.7	11	1.2
+23	12.3	9.3	2	0.0
+24	12.8	9.6	3	0.8
+25	11.2	8.3	2	1.7
+26	12.3	9.4	1	–
+28	11.2	8.4	5	1.7
+29	12.5	9.5	1	–
+30	13.4	9.8	2	0.4
+31	11.2	8.5	1	–
+32	10.0	0.8	3	3.0
+34	11.8	0.8	6	4.4
+35	12.6	0.9	4	4.2
+36	15.7	–0.2	N/A	N/A
+37	12.3	–1.0	N/A	N/A
+38	12.1	7.3	2	0.8
+39	13.0	2.2	3	1.0
+40	12.0	2.1	3	1.8
+41	14.2	1.0	5	1.8
+42	11.4	5.9	2	0.6
+43	12.4	5.9	2	1.1
+45	12.6	1.1	3	1.3
+47	13.2	1.1	5	1.0
+48	13.5	1.5	3	1.1
+49	13.8	1.5	4	2.0
+50	14.3	1.5	4	1.9
+51	12.1	4.2	5	1.1
+52	11.4	5.5	5	0.4
+54	13.2	1.8	4	1.1
+56	15.2	0.9	3	4.8
+57	14.2	0.5	4	8.9
+59	13.9	0.6	5	4.4
+62	11.3	4.8	5	5.0
+64	15.3	3.3	4	2.0
+65	13.8	0.5	5	6.0
+67	12.6	5.3	8	0.6
+69	10.8	3.7	3	0.3
+70	11.3	3.7	6	1.8
+71	11.5	3.7	2	1.1
+72	11.9	3.8	5	0.5
+73	12.1	3.8	5	0.9
+75	16.5	0.7	5	1.8
Prediction set				
#9	14.6	3.1	8	6.1
#17	13.5	2.9	4	1.9
#27	12.6	9.7	3	0.2
#33	11.9	0.8	6	3.8
#44	12.5	6.0	2	1.6
#46	12.9	1.1	4	2.2
#53	10.3	4.2	4	0.6
#55	15.7	0.9	2	3.1
#58	12.7	0.6	5	4.8
#60	15.0	3.2	5	3.8
#61	13.5	0.4	4	10.2
#63	16.8	3.3	5	2.2
#66	11.2	2.1	7	2.1
#68	11.2	3.6	7	0.7
#74	12.3	3.8	6	0.6

EC50, median effective concentration; n_H = Hill coefficient; SDEV = percentage of sample deviation; N/A = not analyzed (n_H values were negative).

was first optimized for simulation of the dose–response relationship of 80% of the nanoparticles in the overall data set (60 data sets), with a good agreement between model estimates and experimental data of 2.3% SDEV, as shown in Figure 4A. The model was tested by the dose–response relationships collected from 20 reports for 10 metal-based ENMs under 38 different environmental conditions, proving that the model is applicable to various combinations of metal-based ENMs and experimental conditions. In optimizing the model, a key parameter was determined, that is, n_H. Combing the predicted value of n_H with any EC*x* value available (in the present study we used the EC50 value because this effect level is most commonly reported), the dose–response relationship of a given metal-based combination of ENMs and experimental conditions may be simulated by combining the output of the quasi-QSAR model and the EC*x* value. The model was tested by an independent set of dose–response relationships collected from 10 literature reports for seven metal-based ENMs, as tested in 14 different environmentally relevant exposure media. The results (Figure 4B) of this model validation show that the model is capable of properly predicting new data sets.

Although the present quasi-QSAR model has been found to be successful for treating many combinations of metal-based ENMs and testing conditions, the model still has limitations. As with any QSAR model, the model is only capable of predicting the response of *D. magna* for metal-based ENMs that were present in the test set (applicability domain) and for which the model was optimized. The same is true with regard to the testing conditions, albeit this is less of a limitation because the ecological niche for daphnids is quite narrow in terms of water properties like pH, DOC, temperature. The boundaries for these water conditions are actually given in OECD guideline 202 (OECD, 2004), and the water conditions used in all tests

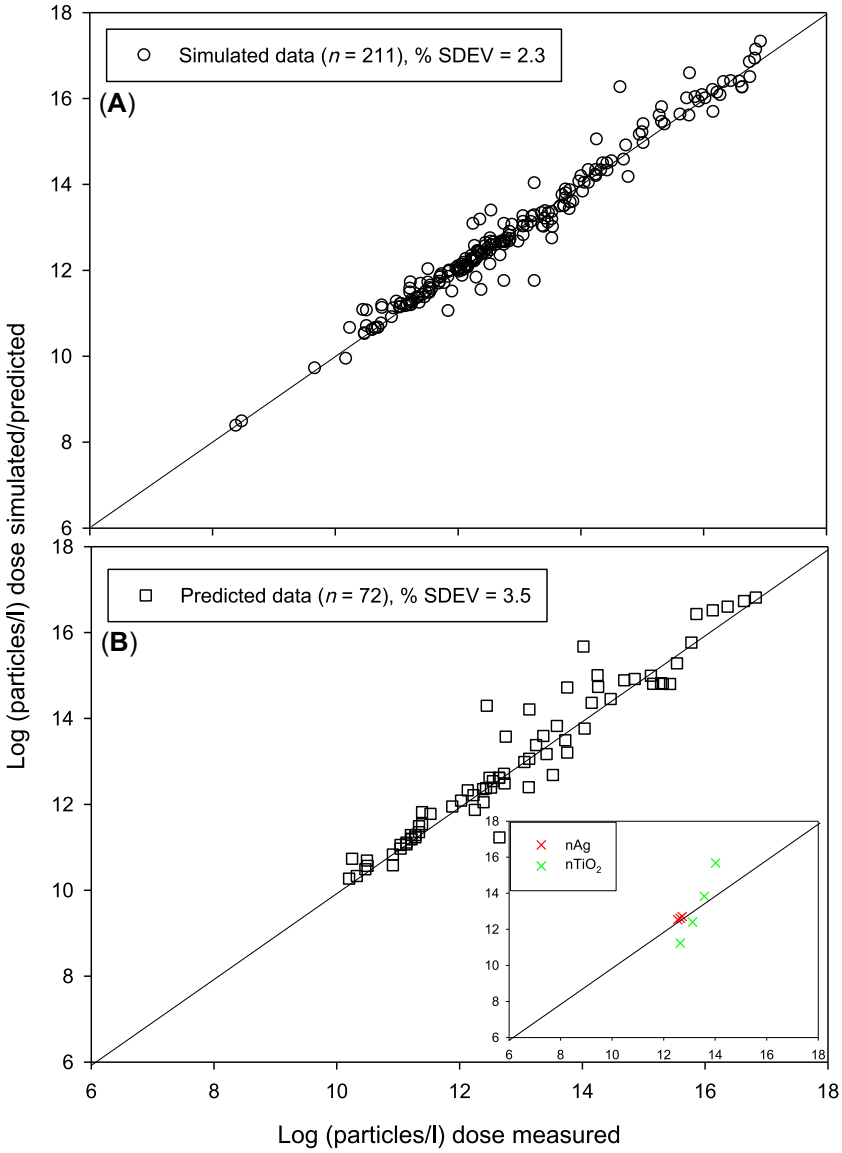

FIGURE 4: Comparison of modeled and measured response data for *Daphnia magna* immobilization, where (**A**) represents the model simulations for 10 metal-based nanomaterials from 20 literature reports (Supporting Information, Table S1) and (**B**) shows model predictions for seven metal-based nanomaterials from 10 literature reports (Supporting Information, Table S2). Inset in (**B**) represents the best predicted (simplified molecular input line entry system, percentage sample deviation [SDEV] = 0.2) case of polyethylene glycol–capped nAg in suspensions of Suwannee River dissolved organic carbon (low concentration) from Newton et al. (2013) and the worst predicted case (% SDEV = 10.2) of $nTiO_2$ (Ø 20 nm) in 10-fold diluted International Organization for Standardization media under simulated solar radiation in a 16:8-h light: dark cycle, as reported by Wyrwoll et al. (2016).

included in the test and validation sets adhered to these boundaries. This implies that the quasi-QSAR model is applicable within these boundaries. As a matter of course, re-optimization with input of new metal-based ENMs is needed when extending the applicability domain by inclusion of ENMs hitherto not included in model development. Another limitation is that the effectiveness of the present model is limited to the EC5 to EC95 range because the experimental noise for data outside of this range is relatively large. It is to be noted explicitly that this is not a shortcoming of the model but a shortcoming of the experimental data commonly reported in the literature.

Prospects of linking the quasi-QSAR model to QSAR models for prediction of effect levels

Various researchers have provided guidance for the proper derivation of EC50 values (see, e.g., Noel et al., 2018; Sebaugh, 2011). Puzyn et al. (2011) used data generated according to this guidance to develop a model to predict effect levels for the cytotoxicity of 17 metal oxide nanoparticles to *Escherichia coli* cells based on the enthalpy of formation of a gaseous cation present in the same oxidation state as that in the metal oxide structure (ΔH_{Me+}). These authors found that values of –log(EC50) were equal to $2.59 - 0.50\Delta H_{Me+}$. Gajewicz et al. (2015) employed a similar approach for estimating –log

(EC50) of 18 nanometal oxides for impacts on a human keratinocyte cell line (HaCaT). In this contribution of Gajewicz et al. (2015), two QSAR descriptors were employed, that is, the enthalpy of formation of a metal oxide nanocluster representing a fragment of the surface (ΔH_f^c) and Mulliken's electronegativity of the cluster (χ^c). It was found that –log(EC50) is equal to 2.47 (±0.05) + 0.24 (±0.05)ΔH_f^c + 0.39 (±0.05) χ^c. Pan et al. (2016) used the data set reported by Gajewicz et al. (2015) to develop two QSAR models in which SMILES-based optimal descriptors were integrated:

$$\log\left(\frac{1}{LC50}\right) = -0.2909(\pm 0.0664) + 0.1038(\pm 0.0027) \times DCW(1,3) \quad (5)$$

with $n = 13$, $R^2 = 0.961$, $Q^2_{LMO} = 0.939$, $s = 0.008$, $F = 268$, $p < 0.0001$.

$$\log\left(\frac{1}{LC50}\right) = 0.0012(\pm 0.0048) + 0.0778(\pm 0.0001) \times DCW(1,3) \quad (6)$$

with $n = 12$, $R^2 = 0.999$, $Q^2_{LMO} = 0.999$, $s = 0.007$, $F = 1273$, $p < 0.0001$.

In these equations, LC50 is the median lethal concentration, n is the number of ENMs in the training set, Q^2_{LMO} is the cross-validated R^2, s is the standard error, F is the Fischer ratio, and p is the p value. The number 1 in DCW(1,3) is the coefficient for categorization of features into two groups (noise and active); the number 3 in DCW(1,3) is the number of epochs of the Monte Carlo optimization. In addition, Pan et al. (2016) employed the same approach with the data set reported by Puzyn et al. (2011) and developed a model that can be expressed as follows:

$$\log\left(\frac{1}{LC50}\right) = 0.0321(\pm 0.1443) + 0.2658(\pm 0.0141) \times DCW(6,11) \quad (7)$$

with $n = 10$, $R^2 = 0.889$, $Q^2_{LMO} = 0.838$, $s = 0.179$, $F = 164$, $p < 0.0001$.

$$\log\left(\frac{1}{LC50}\right) = -0.0076(\pm 0.0306) + 0.1420(\pm 0.0020) \times DCW(6,17) \quad (8)$$

with $n = 9$, $R^2 = 0.982$, $Q^2_{LMO} = 0.975$, $s = 0.007$, $F = 391$, $p < 0.0001$.

OUTLOOK FOR ENVIRONMENTAL EFFECT ASSESSMENT

The quasi-QSAR model that we developed quantifies the relationship between the dose of a metallic nanoparticle to which the daphnid *D. magna* is exposed and the immobilization response with an accuracy (SDEV) of on average 2.1%. If experimental values of any ECx level under any kind of testing or exposure conditions are available, the full dose–response curve of the metallic nanoparticle can be estimated. The quasi-QSAR model can also be used as a building block to connect to QSAR-like comprehensive models developed recently, allowing one to calculate an ECx of ENMs from a cryptography based on the Monte Carlo optimization (Cao et al., 2020; Pan et al., 2016; Toropova et al., 2015, 2017) and regression-based QSAR models (Gajewicz et al., 2015; Kar et al., 2014; Mu et al., 2016; Pathakoti et al., 2014; Puzyn et al., 2011). These models are instrumental for screening the nano-safety of metal-based nanomaterials that are not intensively tested or are tested at new exposure conditions. This is needed to perform a robust environmental effect assessment for nanomaterials. Prospects of this type of model can also be found in the development of these quasi-QSAR models for other aquatic organisms that are commonly used in risk assessment.

Supporting Information—The Supporting Information is available on the Wiley Online Library at https://doi.org/10.1002/etc.5322.

Acknowledgment—This project has received funding from the European Union's Horizon 2020 research and innovation program under grant 814426 (NanoInformaTIX).

Data Availability Statement—Data, associated metadata, and calculation tools are available from the corresponding author (willie.peijnenburg@rivm.nl).

REFERENCES

Briffa, S., Nasser, F., Valsami-Jones, E., & Lynch, I. (2018). Uptake and impacts of polyvinylpyrrolidone (PVP) capped metal oxide nanoparticles on *Daphnia magna*: Role of core composition and acquired corona. *Environmental Science: Nano*, *5*, 1745–1756.

Cao, J., Pan, Y., Jiang, Y., Qi, R., Yuan, B., Jia, Z., Jiang, J., & Wang, Q. (2020). Computer-aided nanotoxicology: Risk assessment of metal oxide nanoparticles via nano-QSAR. *Green Chemistry*, *22*, 3512–3521.

Carnesecchi, E., Toropov, A. A., Toropova, A. P., Kramer, N., Svendsen, C., Dorne, J. L., & Benfenati, E. (2020). Predicting acute contact toxicity of organic binary mixtures in honey bees (*A. mellifera*) through innovative QSAR models. *Science of the Total Environment*, *704*, Article 135302.

Chatterjee, A. K., Chakraborty, R., & Basu, T. (2014). Mechanism of antibacterial activity of copper nanoparticles. *Nanotechnology*, *25*, Article 135101.

Chen, G., Vijver, M. G., & Peijnenburg, W. J. (2015). Summary and analysis of the currently existing literature data on metal-based nanoparticles published for selected aquatic organisms: Applicability for toxicity prediction by (Q)SARs. *Alternatives to Laboratory Animals*, *43*, 221–240.

Chevalier, J. (2014). *Utilisation du comportement natatoire de Daphnia magna comme indicateur sensible et précoce de toxicité pour l'évaluation de la qualité de l'eau* [Unpublished doctoral dissertation]. Université de Bordeaux.

Choi, J.-S., Trinh, T. X., Yoon, T.-H., Kim, J., & Byun, H.-G. (2019). Quasi-QSAR for predicting the cell viability of human lung and skin cells exposed to different metal oxide nanomaterials. *Chemosphere*, *217*, 243–249.

Crittenden, J. C., Sanongraj, S., Bulloch, J. L., Hand, D. W., Rogers, T. N., Speth, T. F., & Ulmer, M. (1999). Correlation of aqueous-phase adsorption isotherms. *Environmental Science & Technology*, *33*, 2926–2933.

Cui, R., Chae, Y., & An, Y.-J. (2017). Dimension-dependent toxicity of silver nanomaterials on the cladocerans *Daphnia magna* and *Daphnia galeata*. *Chemosphere*, *185*, 205–212.

Cupi, D., Hartmann, N. B., & Baun, A. (2016). Influence of pH and media composition on suspension stability of silver, zinc oxide, and titanium dioxide nanoparticles and immobilization of *Daphnia magna* under guideline testing conditions. *Ecotoxicology and Environmental Safety*, *127*, 144–152.

Dabrunz, A., Duester, L., Prasse, C., Seitz, F., Rosenfeldt, R., Schilde, C., Schaumann, G. E., & Schulz, R. (2011). Biological surface coating and molting inhibition as mechanisms of TiO_2 nanoparticle toxicity in *Daphnia magna*. *PLoS One*, *6*, Article e20112.

Farner, J. M., Cheong, R. S., Mahé, E., Anand, H., & Tufenkji, N. (2019). Comparing TiO_2 nanoparticle formulations: Stability and photoreactivity are key factors in acute toxicity to *Daphnia magna*. *Environmental Science: Nano*, *6*, 2532–2543.

Gajewicz, A., Schaeublin, N., Rasulev, B., Hussain, S., Leszczynska, D., Puzyn, T., & Leszczynski, J. (2015). Towards understanding mechanisms governing cytotoxicity of metal oxides nanoparticles: Hints from nano-QSAR studies. *Nanotoxicology*, *9*, 313–325.

Gao, X., Deng, R., & Lin, D. (2020). Insights into the regulation mechanisms of algal extracellular polymeric substances secretion upon the exposures to anatase and rutile TiO_2 nanoparticles. *Environmental Pollution*, *263*, Article 114608.

Goldbeter, A., & Dupont, G. (1990). Allosteric regulation, cooperativity, and biochemical oscillations. *Biophysical Chemistry*, *37*, 341–353.

Heggelund, L. R., Diez-Ortiz, M., Lofts, S., Lahive, E., Jurkschat, K., Wojnarowicz, J., Cedergreen, N., Spurgeon, D., & Svendsen, C. (2014). Soil pH effects on the comparative toxicity of dissolved zinc, non-nano and nano ZnO to the earthworm *Eisenia fetida*. *Nanotoxicology*, *8*, 559–572.

Heinlaan, M., Ivask, A., Blinova, I., Dubourguier, H.-C., & Kahru, A. (2008). Toxicity of nanosized and bulk ZnO, CuO and TiO_2 to bacteria *Vibrio fischeri* and crustaceans *Daphnia magna* and *Thamnocephalus platyurus*. *Chemosphere*, *71*, 1308–1316.

Hill, A. V. (1910). The possible effects of the aggregation of the molecules of haemoglobin on its dissociation curves. *Journal of Physiology*, *40*, 4–7.

Honary, S., & Zahir, F. (2013a). Effect of zeta potential on the properties of nano-drug delivery systems—A review (Part 1). *Tropical Journal of Pharmaceutical Research*, *12*, 255–264.

Honary, S., & Zahir, F. (2013b). Effect of zeta potential on the properties of nano-drug delivery systems—A review (Part 2). *Tropical Journal of Pharmaceutical Research*, *12*, 265–273.

International Organization for Standardization. (2012). *Water quality—Determination of the inhibition of the mobility of Daphnia magna Straus (Cladocera, Crustacea)—Acute toxicity test* (ISO 6341:2012).

Jantunen, A. P. K., Gottardo, S., Rasmussen, K., & Crutzen, H. P. (2018). An inventory of ready-to-use and publicly available tools for the safety assessment of nanomaterials. *NanoImpact*, *12*, 18–28.

Kar, S., Gajewicz, A., Puzyn, T., Roy, K., & Leszczynski, J. (2014). Periodic table–based descriptors to encode cytotoxicity profile of metal oxide nanoparticles: A mechanistic QSTR approach. *Ecotoxicology and Environmental Safety*, *107*, 162–169.

Kim, S., Samanta, P., Yoo, J., Kim, W.-K., & Jung, J. (2017). Time-dependent toxicity responses in *Daphnia magna* exposed to CuO and ZnO nanoparticles. *Bulletin of Environmental Contamination and Toxicology*, *98*, 502–507.

Lee, Y. J., Kim, J., Oh, J., Bae, S., Lee, S., Hong, I. S., & Kim, S. H. (2012). Ion-release kinetics and ecotoxicity effects of silver nanoparticles. *Environmental Toxicology and Chemistry*, *31*, 155–159.

Li, X., Schirmer, K., Bernard, L., Sigg, L., Pillai, S., & Behra, R. (2015). Silver nanoparticle toxicity and association with the alga *Euglena gracilis*. *Environmental Science: Nano*, *2*, 594–602.

Ma, H., Brennan, A., & Diamond, S. A. (2012). Phototoxicity of TiO_2 nanoparticles under solar radiation to two aquatic species: *Daphnia magna* and Japanese medaka. *Environmental Toxicology and Chemistry*, *31*, 1621–1629.

Metropolis, N., & Ulam, S. (1949). The Monte Carlo method. *Journal of the American Statistical Association*, *44*, 335–341.

Mu, Y., Wu, F., Zhao, Q., Ji, R., Qie, Y., Zhou, Y., Hu, Y., Pang, C., Hristozov, D., & Giesy, J. P. (2016). Predicting toxic potencies of metal oxide nanoparticles by means of nano-QSARs. *Nanotoxicology*, *10*, 1207–1214.

Newton, K. M., Puppala, H. L., Kitchens, C. L., Colvin, V. L., & Klaine, S. J. (2013). Silver nanoparticle toxicity to *Daphnia magna* is a function of dissolved silver concentration. *Environmental Toxicology and Chemistry*, *32*, 2356–2364.

Noel, Z. A., Wang, J., & Chilvers, M. I. (2018). Significant influence of EC50 estimation by model choice and EC50 type. *Plant Disease*, *102*, 708–714.

Oleszczuk, P., śJośko, I., & Skwarek, E. (2015). Surfactants decrease the toxicity of ZnO, TiO_2 and Ni nanoparticles to *Daphnia magna*. *Ecotoxicology*, *24*, 1923–1932.

Oomen, A. G., Steinhäuser, K. G., Bleeker, E. A. J., van Broekhuizen, F., Sips, A., Dekkers, S., Wijnhoven, S. W. P., & Sayre, P. G. (2018). Risk assessment frameworks for nanomaterials: Scope, link to regulations, applicability, and outline for future directions in view of needed increase in efficiency. *NanoImpact*, *9*, 1–13.

Organisation for Economic Co-operation and Development. (2004). Test No. 202: *Daphnia* sp. acute immobilisation test. *OECD guidelines for the testing of chemicals*.

Organisation for Economic Co-operation and Development. (2020). *Guidance document for the testing of dissolution and dispersion stability of nanomaterials and the use of the data for further environmental testing and assessment strategies*. Series on Testing and Assessment No. 318 (ENV/JM/MONO(2020)9).

Pan, Y., Li, T., Cheng, J., Telesca, D., Zink, J. I., & Jiang, J. (2016). Nano-QSAR modeling for predicting the cytotoxicity of metal oxide nanoparticles using novel descriptors. *RSC Advances*, *6*, 25766–25775.

Panzarini, E., Mariano, S., Carata, E., Mura, F., Rossi, M., & Dini, L. (2018). Intracellular transport of silver and gold nanoparticles and biological responses: An update. *International Journal of Molecular Sciences*, *19*, Article 1305.

Pathakoti, K., Huang, M.-J., Watts, J. D., He, X., & Hwang, H.-M. (2014). Using experimental data of *Escherichia coli* to develop a QSAR model for predicting the photo-induced cytotoxicity of metal oxide nanoparticles. *Journal of Photochemistry and Photobiology, B: Biology*, *130*, 234–240.

PubChem. (2021). https://pubchem.ncbi.nlm.nih.gov/

Puzyn, T., Rasulev, B., Gajewicz, A., Hu, X., Dasari, T. P., Michalkova, A., Hwang, H.-M., Toropov, A., Leszczynska, D., & Leszczynski, J. (2011). Using nano-QSAR to predict the cytotoxicity of metal oxide nanoparticles. *Nature Nanotechnology*, *6*, 175–178.

Rubinstein, R. Y., & Kroese, D. P. (2016). *Simulation and the Monte Carlo method*. John Wiley & Sons.

Santos-Rasera, J. R., Neto, A. S. A., Monteiro, R. T. R., Van Gestel, C. A., & De Carvalho, H. W. P. (2019). Toxicity, bioaccumulation and biotransformation of Cu oxide nanoparticles in *Daphnia magna*. *Environmental Science: Nano*, *6*, 2897–2906.

Schiwy, A., Maes, H. M., Koske, D., Flecken, M., Schmidt, K. R., Schell, H., Tiehm, A., Kamptner, A., Thümmler, S., Stanjek, H., Heggen, M., Dunin-Borkowski, R. E., Braun, J., Schäffer, A., & Hollert, H. (2016). The ecotoxic potential of a new zero-valent iron nanomaterial, designed for the elimination of halogenated pollutants, and its effect on reductive dechlorinating microbial communities. *Environmental Pollution*, *216*, 419–427.

Sebaugh, J. (2011). Guidelines for accurate EC50/IC50 estimation. *Pharmaceutical Statistics*, *10*, 128–134.

Seo, J., Kim, S., Choi, S., Kwon, D., Yoon, T.-H., Kim, W.-K., Park, J.-W., & Jung, J. (2014). Effects of physiochemical properties of test media on nanoparticle toxicity to *Daphnia magna straus*. *Bulletin of Environmental Contamination and Toxicology*, *93*, 257–262.

Song, L., Vijver, M. G., de Snoo, G. R., & Peijnenburg, W. J. (2015). Assessing toxicity of copper nanoparticles across five cladoceran species. *Environmental Toxicology and Chemistry*, *34*, 1863–1869.

Sovová, T., Kocí, V., & Kochánková, L. (2009). Ecotoxicity of nano and bulk forms of metal oxides. In *Conference proceedings—NANOCON 2009* (pp. 62–71). Tanger.

Strigul, N., Vaccari, L., Galdun, C., Wazne, M., Liu, X., Christodoulatos, C., & Jasinkiewicz, K. (2009). Acute toxicity of boron, titanium dioxide, and aluminum nanoparticles to *Daphnia magna* and *Vibrio fischeri*. *Desalination*, *248*, 771–782.

Toropov, A. A., Toropova, A. P., Martyanov, S. E., Benfenati, E., Gini, G., Leszczynska, D., & Leszczynski, J. (2011). Comparison of SMILES and molecular graphs as the representation of the molecular structure for QSAR analysis for mutagenic potential of polyaromatic amines. *Chemometrics and Intelligent Laboratory Systems*, *109*, 94–100.

Toropov, A. A., Toropova, A. P., Martyanov, S. E., Benfenati, E., Gini, G., Leszczynska, D., & Leszczynski, J. (2012). CORAL: Predictions of rate constants of hydroxyl radical reaction using representation of the molecular structure obtained by combination of SMILES and graph approaches. *Chemometrics and Intelligent Laboratory Systems*, *112*, 65–70.

Toropova, A. P., Toropov, A. A., Benfenati, E., Gini, G., Leszczynska, D., & Leszczynski, J. (2011). CORAL: Quantitative structure–activity relationship models for estimating toxicity of organic compounds in rats. *Journal of Computational Chemistry*, *32*, 2727–2733.

Toropova, A. P., Toropov, A. A., Leszczynska, D., & Leszczynski, J. (2017). CORAL and Nano-QFAR: Quantitative feature–activity relationships (QFAR) for bioavailability of nanoparticles (ZnO, CuO, Co_3O_4, and TiO_2). *Ecotoxicology and Environmental Safety*, *139*, 404–407.

Toropova, A. P., Toropov, A. A., Martyanov, S. E., Benfenati, E., Gini, G., Leszczynska, D., & Leszczynski, J. (2012). CORAL: QSAR modeling of toxicity of organic chemicals towards *Daphnia magna*. *Chemometrics and Intelligent Laboratory Systems*, *110*, 177–181.

Toropova, A. P., Toropov, A. A., Rallo, R., Leszczynska, D., & Leszczynski, J. (2015). Optimal descriptor as a translator of eclectic data into prediction of cytotoxicity for metal oxide nanoparticles under different conditions. *Ecotoxicology and Environmental Safety*, *112*, 39–45.

Wyrwoll, A. J., Lautenschläger, P., Bach, A., Hellack, B., Dybowska, A., Kuhlbusch, T. A., Hollert, H., Schäffer, A., & Maes, H. M. (2016). Size matters—The phototoxicity of TiO_2 nanomaterials. *Environmental Pollution*, *208*, 859–867.

Xiao, Y., Peijnenburg, W. J. G. M., Chen, G., & Vijver, M. G. (2016). Toxicity of copper nanoparticles to *Daphnia magna* under different exposure conditions. *Science of the Total Environment*, *563–564*, 81–88.

Xiao, Y., Vijver, M. G., Chen, G., & Peijnenburg, W. J. (2015). Toxicity and accumulation of Cu and ZnO nanoparticles in *Daphnia magna*. *Environmental Science & Technology*, *49*, 4657–4664.

Yang, S., Ye, R., Han, B., Wei, C., & Yang, X. (2014). Ecotoxicological effect of nano-silicon dioxide particles on *Daphnia magna*. *Integrated Ferroelectrics*, *154*, 64–72.

